Formation of anomalous optomagnetic resonances in neon in the transition $3s_2-2p_4$

É. G. Saprykin, S. N. Seleznev, and V. A. Sorokin

Institute of Automation and Electrometry, Siberian Branch, Russian Academy of Sciences
(Submitted 12 November 1991; resubmitted 26 February 1992)
Zh. Eksp. Teor. Fiz. **102**, 14–25 (July 1992)

By scanning a transverse magnetic field, anomalously narrow optomagnetic resonances ($\lambda = 0.63\,\mu$m) with unusual amplitude-dispersive properties were observed in neon. Their collision characteristics were measured and the range of gas pressures at which such resonances appear was established. Their behavior in an additional longitudinal magnetic field was also studied. Using the experimental data, a phenomenological theory for the formation of optomagnetic resonances with anomalous properties was formulated.

1. INTRODUCTION

In Refs. 1 and 2, we first reported the observation of unusual optomagnetic resonances (OMR) during the scanning of a transverse magnetic field. In the well-known neon transition $3s_2-2p_4$, under conditions of linear absorption, we recorded resonances which were essentially different in their dispersive and relaxation properties from the OMR observed earlier[4] in the same transition.

In the present work, we investigated the polarization symmetry of the OMR and the range of gas pressures at which they appear. We also established at higher accuracy their relaxation properties, and investigated the effect of an additional longitudinal magnetic field. The experimental results led us to the conclusion that one deals with two radically different types of optomagnetic resonances. By varying the experimental conditions, we found that the properties of these two types of resonances are sharply different. The first type are OMR with normal properties that depend on the parameters of the considered transition. The second are anomalous OMR, the source of which is as yet unclear.

The experimental data on amplitude-dispersive, relaxation, and polarization properties of OMR are reported in Sec. 2. They refer to OMR-dichroism and OMR-birefringence recorded simultaneously, under identical experimental conditions, using an automated two-channel Zeeman spectrometer.

In Sec. 3 we describe a qualitative phenomenological theory of the properties of OMR formed with different types of excitation symmetry of the levels under consideration. We show that there exists an excitation anisotropy, under which OMR are formed with anomalous properties similar to those observed experimentally.

Some notation is necessary to facilitate the description of the experimental data and of the calculation results. Irrespective of the magnetooptic dichroism or birefringence, we shall denote by OMR-1 the resonances of the first ("usual") type, and by OMR-2 those of the second ("anomalous") type. The dichroism or the birefringence will be labeled a subscript a or n. For example, OMR_a-1 will mean an OMR of first type in dichroism, and OMR_n-2 and OMR of second type in birefringence.

2. EXPERIMENTALLY OBSERVABLE OMR-1 AND OMR-2 PROPERTIES

The OMR were recorded using an automated Zeeman spectrometer with transverse orientation of the scanning magnetic field. In order to realize an appropriate method of Zeeman spectroscopy, we added an alternating component to the scanned field. To eliminate the effect of external magnetic fields, we superimposed on the gas discharge neon cell additional fields, one longitudinal and one transverse, perpendicular to the scanned field.

As a probing source of circular polarization we used a monochromatic He–Ne laser with a controllable generating frequency.

The measurement procedure was based on an analysis of the polarization ellipse of the transmitted light. Under the action of the transverse magnetic field, the gas became dichroic and birefringent. As a result, the difference between the intensities of the beams separated by a polarizing prism (e.g. of Frank–Ritter type) is given by the expression

$$S=S_a+S_n=[E_1^2\exp(-2lkn_\perp'')-E_2^2\exp(-2lkn_\parallel'')]\cos 2\varphi + 2E_1E_2\sin 2\varphi\cos[kl(n_\perp'-n_\parallel')+\psi_0]\exp[-lk(n_\parallel''+n_\perp'')]. \quad (1)$$

Here S is the total signal, S_a is the dichroism signal, S_n is the birefringence signal, $n_\parallel = n_\parallel' + in_\parallel''$ and $n_\perp = n_\perp' + in_\perp''$ are the complex refractive indices of the normal waves polarized parallel and perpendicular to the transverse magnetic field $H_\perp$, φ is the angle between the polarization prism and $H_\perp$, ψ_0 is the initial phase shift of the wave components, E_1 and E_2 are the initial amplitudes, and l is the path length in the medium. The circular polarization of the radiation is best suited for separating OMR_a or OMR_n, provided the angle φ equals either 0° or 45°. In our experiments, OMR_a and OMR_n were recorded simultaneously, by splitting the transmitted beam into two components analyzed by two polarization prisms.

In Ref. 2 we have already reported on some properties of OMR. OMR-1 was completely explained as due to alignment on the $2p_4$ level by the excitation anisotropy in the cylindrical gas-discharge cell. The collisional properties of

 0038-5646/92/070008-06$05.00

OMR-1 (neon pressure broadening) could be accurately described by the relaxation parameters of the $2p_4$ level.

The amplitude-dispersive properties of OMR-1 are in agreement with classical dispersion theory. The OMR_a-1 amplitude is a maximum at the center of the absorption line, decreasing symmetrically towards the red and blue wings of the probing radiation. OMR_n-1 vanishes correspondingly at the center of the absorption profile. Detuning of the radiation frequency by about $k\bar{v}$ (k is the wave vector and $\bar{v}$ the average thermal velocity) maximizes the amplitude of OMR_n-1, although the signs in the red and blue wings are different.

The properties of OMR-2 proved to be altogether unusual. Firstly, the resonance widths in magnetic-field units were less than 0.3 G, which is almost an order of magnitude smaller than the widths of OMR-1. They can hardly be related to any decay to the $2p_4$ and $3s_2$ levels, since the widths of these levels equal 8 MHz even in spontaneous relaxation, which gives a value of 2.5 G, almost an order of magnitude larger [the Landé g-factors for the $3s_2$ and $2p_4$ levels are practically the same, both equal to 1.3 (Ref. 3)]. In the following we shall use magnetic units, since the Landé g-factor for OMR-2 is not known. Secondly, OMR-2 have paradoxical amplitude dispersive properties. OMR_n-2 does not vanish at the center of the absorption line. Moreover, its amplitude is practically independent of the frequency of the probing radiation in the investigated range from -500 MHz to $+300$ MHz. As a consequence of the dispersion relations, OMR_a-2 is not observed (in a purely transverse field).

The anomalous characteristics of OMR-2 compelled us to look first for all for possible technical causes of these unusual resonances. One might assume that OMR-2 is a manifestation of distorted OMR-1 with smaller width. The reduced width might be related to a scale change of the magnetic field in the neighborhood of the zero-field point, due to technical reasons such as nonlinear scanning or amplitude modulation. The strange amplitude-dispersive properties could be a consequence of dichroism and birefringence signal mixing induced by prism defects or inaccurate adjustments.

We tested several types of discharge cells and electromagnets, varying the optical components of the apparatus, and the electronic and control units. Invariably, the experimental results were qualitatively the same. The final experimental setup and its separate elements were free of scanning or modulation defects.

The electromagnet and the cell were made of nonmagnetic materials, ensuring linearity of the electromagnet current in the magnetic field. The winding geometry was such that the nonuniformities of the magnetic field were outside the discharge region. The screening of the external magnetic field by means of passive ferromagnetic elements proved to be ineffective because of the interaction between the electromagnet and the screen. As a result, in the region of zero fields, one could observe a rotation of the scanning plane by an angle up to 90°, which caused a mixing of the OMR_a-1 and OMR_n-2 signals. The effect of the external field was reduced by means of a compensating procedure. The uniformity of the magnetic field was checked against the OMR parameters recorded in one-fifth of the discharge cell, using additional modulation coils movable along the cell. The modulation amplitude of the magnetic field was controlled and maintained constant within 5%. The remaining nonuniformity, 0.05 G, manifested itself in the form of a nonmonotonic magnetic broadening of OMR_a-2 (see Fig. 4, curve *2*, below). Another manifestation of nonuniformity was the overestimate of the OMR_p-2 widths.

The polarization Frank–Ritter prisms employed to separate the OMR_a and OMR_n signals had a light attenuation coefficient of 0.1%. The prism axis was aligned with respect to the transverse magnetic field with an error of less than 5°, which according to (1) gives for the signal mixing a value of about 1.5%. In the course of adjustment of the installation, we intentionally misaligned the prisms, and observed in one channel the mixing of the dichroism and birefringence signals, as described by formula (1). All electronic amplifiers and converters had a better than 0.1% linearity.

Thus, all results obtained in testing the apparatus for scanning and registration refute the hypothesis that OMR-2 are of technical origin. There exist also other compelling reasons to refute an apparatus-dependent origin. The curves *1* and *2* in Fig. 1 show the derivatives of OMR_a-1 and OMR_n-2 at the center of the absorption line as functions of the neon pressure. Curve *1* reaches a maximum at about 0.7–1.0 torr, then decreases asymptotically. A similar behavior was demonstrated[4] for pressures up to 4.5 torr. We went even farther, up to 8.5 torr, and verified the increasing role[4] of anisotropic collisions ("wind effect") in level alignment at high gas pressures. Curve *2* shows the existence domain of OMR-2. Its maximum appears at visibly lower pressures than for OMR-1. Its amplitude decreases sharply as the pressure increases and OMR_n-2 practically disappears completely at pressures higher than 4.5 torr. On the basis of these data alone, one can conclude that OMR-1 and OMR-2 have entirely different origins.

Preliminary data concerning the relaxation properties of OMR-2 have already been reported.[2] The curves *3* and *4*

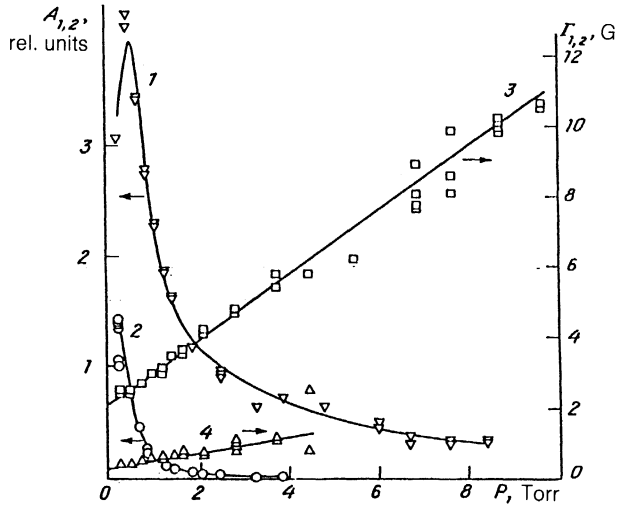

FIG. 1. Amplitude (*1*) and width (*3*) of OMR_a-1 vs neon pressure. Curves *2* and *4* show the domain of existence and the collisional broadening of OMR_n-2. The data were obtained at the center of the absorption line for a discharge current of 90 mA.

from Fig. 1 give a more precise description of the relaxation properties of OMR-1 and OMR-2. Curve *3* characterizes the collisional broadening of the alignment constant for the level $2p_4$, and is well approximated by the linear function:

$$\Gamma_1=\gamma_1+(\partial\Gamma_1/\partial P)P=(2{,}11\pm0{,}02)\ [\text{G}]$$
$$+(0{,}913\pm0{,}012)\ [\text{G/Torr}]\cdot P.$$

The broadening parameter $\partial\Gamma_1/\partial P$ and the decay rate γ_1 in the spontaneous limit are fairly well known,[4-6] and are given here only for purposes of comparison with the OMR-2 collisional broadening. The latter is given by the following approximation:

$$\Gamma_2=\gamma_2+(\partial\Gamma_2/\partial P)P=(0{,}271\pm0{,}012)\ [\text{G}]$$
$$+(0{,}225\pm0{,}015)\ [\text{G/Torr}]\cdot P.$$

Note that the curves *3* and *4* are not related by a scale transformation. This is additional evidence that OMR-2 is an independent physical effect.

The small width of OMR-2 in magnetic units manifested itself in control measurements involving the application of an additional longitudinal magnetic field. On the left side of Fig. 2 we show the evolution of OMR_n-1 and OMR_n-2 as the longitudinal magnetic field $H_\parallel$ varies from $+0.6$ to -1 G. The scale of the magnetic field is proportional to the current in the solenoid surrounding the cell. On the right side of the figure we give the variation of the shapes of OMR_a-1 and OMR_a-2 under the same conditions. These graphs were obtained near the center of the absorption line.

We call attention to some typical OMR variations. OMR_n-2 has a maximum amplitude at $H_\parallel=0$, then the amplitude decreases as $|H_\parallel|$ increases, and for $|H_\parallel|>0.5$ G there appears a region with a complex binary structure of OMR_n-2. For weaker longitudinal fields, when a double structure has not yet appeared, the field $H_\parallel$ has a broadening effect. The effect of $H_\parallel$ on OMR_n-1 is noticeably present only in the amplitude and is similar to the effect of retuning the laser frequency.

The changes in OMR_a-1 and OMR_a-2 are somewhat different. In the absence of $H_\parallel$, the OMR_a-2 amplitude equals zero. A weak longitudinal fields leads to the appearance of a narrow component, with an amplitude proportional to the field $H_\parallel$. The sign of OMR_a-2 depends on the direction of the field $H_\parallel$. Note that the OMR_a-2 widths are almost always smaller than those of OMR_n-2. As the absolute value of $H_\parallel$ increases, the OMR_a-2 broadens. The effect of a longitudinal field on OMR_a-1 is hardly visible against the background of the strong initial strong signal.

Note that the zero value of the longitudinal field (on the average along the cell) was reached at a nonzero solenoidal current. It was determined from symmetry considerations. In a purely transverse field, OMR_a should be insensitive to a polarization change from right circular to left circular. It was observed (see curves *3* and *3'* in Fig. 3) that reversal of the type of polarization reverses the sign of OMR_a-2 if its amplitude is not zero. Therefore, the zero of the longitudinal field must be reached at zero amplitude of the narrow part of OMR_a.

The effect of the longitudinal field can be seen in more detail in Fig. 3, in which the curves are the result of a more detailed processing of a series of magnetospectrograms, just as in Fig. 2. As an approximation model, we used the derivative of a linear combination of two Lorentzians, one broad, corresponding to OMR-1, and one narrow, for OMR-2. The curves marked by numbers without primes were obtained for one circular polarization. Those marked by primed numbers correspond to the orthogonal circular polarization.

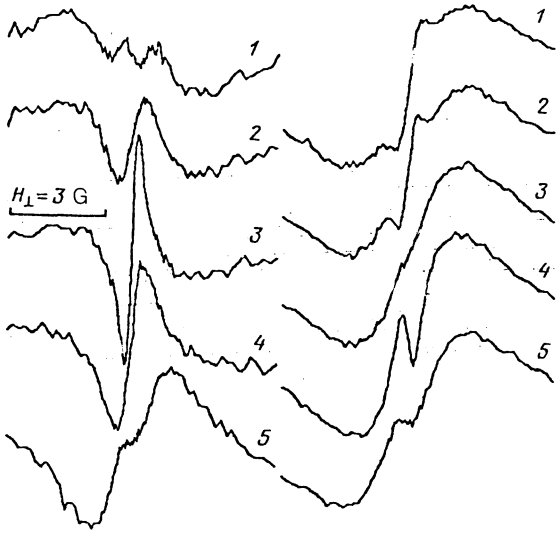

FIG. 2. Evolution of OMR_n (left) and OMR_a (right) in an additional longitudinal field. Curves *1*, *2*, *3*, *4*, and *5* correspond to additional longitudinal fields 0.56, 0.33, 0, -0.35, and 0.95 G.

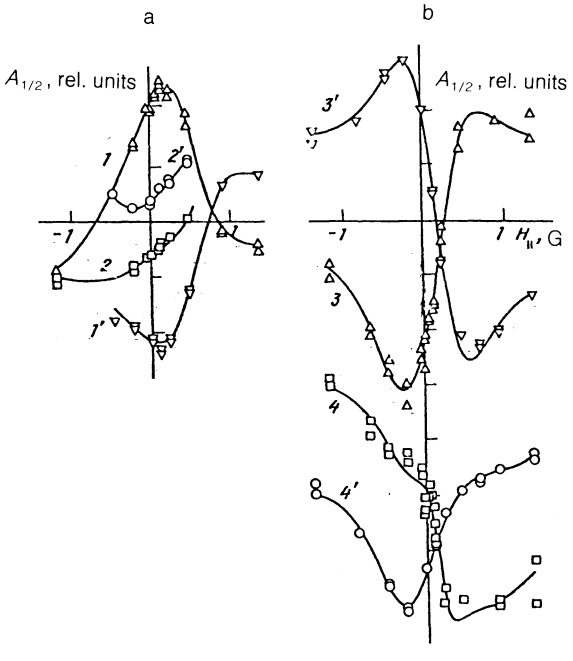

FIG. 3. a—Amplitudes of OMR_n-1 (*1,1'*) and OMR_n-2 (*2,2'*) vs longitudinal magnetic field. b—Amplitudes of OMR_a-1 (*3,3'*) and OMR_a-2 (*4, 4'*) vs longitudinal magnetic field. The primed numbers correspond to one circular polarization, and those without primes to the orthogonal circular polarization.

A change of polarization has different effects on the amplitudes of the broad and narrow parts of OMR. The signs of both OMR_n-2 and OMR_a-2 change. In OMR_n-1 and OMR_a-1 there are parts which change sign and parts which do not. The unit on the abscissa in Fig. 3 is proportional to the current in the solenoid generating the longitudinal magnetic field. For both types of polarization, there exist values of $H_\parallel$ at which OMR_a-2 vanishes. At these values, the narrow part of OMR_n has a maximum amplitude. In these cases, the nonvanishing solenoidal current must generate a compensating longitudinal magnetic field. However, the curves in Fig. 3 are not completely symmetric with respect to the change in sign of the longitudinal magnetic field. The compensating fields for the curves *3* and *3'* are somewhat different, and this difference exceeds the experimental error. On the average, the compensating field is 0.25 G and corresponds to the intersection points of curves *3* with *3'* and *4* with *4'*. In addition to the shifts of the zeros of OMR_a-2 zero, one can also notice a small difference in the OMR amplitudes when the direction of the longitudinal field is reversed. The nature of this difference will be explained in Sec. 3 for OMR-1, but it is still not clear for OMR-2.

The variation of the OMR-2 width with the longitudinal field is given in Fig. 4. For OMR_n-2, up to the appearance of a double structure, one can observe only a broadening. At the beginning, OMR_a-2 narrows somewhat, and then broadens. A characteristic change in the shape of OMR-2 occurs at values of the longitudinal field corresponding to the widths of resonances in a purely transverse magnetic field.

We have thus observed a number of unusual experimental facts, which allow us to conclude that the appearance of OMR-2 cannot be due to apparatus effects. We must accept the fact that the formation of OMR-2 is due to as yet unknown properties of a gas discharge plasma.

3. PHENOMENOLOGICAL THEORY OF OMR

In this section we will define the excitation conditions under which OMR-2 may be observed, we will explain their dispersive and polarization properties, and we will describe their behavior under the action of a longitudinal field. We will also compare their properties with those of OMR-1.

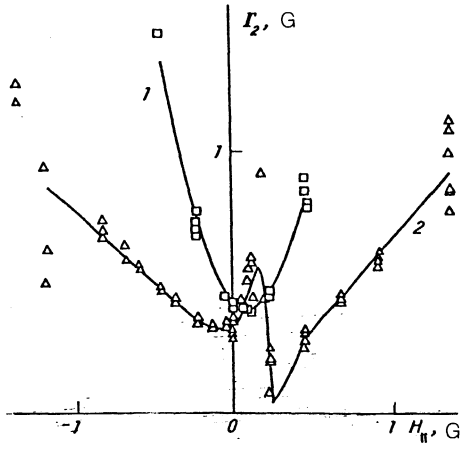

FIG. 4. Broadening of OMR_n-2 (*1*) and OMR_a-2 (*2*) by a longitudinal magnetic field.

Assume that a monochromatic electromagnetic wave propagates in a gas with two energy levels, characterized by the projections J_a and J_b of the angular momentum along the x-axis. The population of these levels will be considered anisotropic, because of alignment. For simplicity, the relaxation characteristics of the levels a and b will be taken to be identical. A magnetic field with a transverse component H_z and a longitudinal component H_x will be assumed to lie in the xz-plane.

The calculations can be conveniently done in the representation of irreducible spherical tensor operators, i.e., in the $\varkappa q$ representation.[7] We introduce two systems of coordinates. In the k system, with the z-axis along $H_\perp$, we shall calculate the optical properties of the gas. In the H system, with a $\tilde{z}$-axis directed along the total magnetic field, it will be convenient to solve the system of equations for the density matrix, because in this system the magnetic field operator is diagonal. The transformation from one system to another is via rotation through an angle β, where $\cos\beta = H_\perp/(H_\perp^2 + H_\parallel^2)^{1/2}$. In the k-system the operator of dipole interaction between an atom and radiation has, in the $\varkappa q$ representation, the components:

$$\mathbf{E}d_{ab} = V_{ab}(1q) = \left(\frac{-iW}{2^{1/2}}, U, \frac{-iW}{2^{1/2}}\right), \tag{2}$$

in which d_{ab} is the reduced dipole moment, and W and U are proportional components of the electric field of the radiation in spherical coordinates. In the case of circular polarization, there is a $\pi/2$ phase shift between W and U, so that it is necessary to replace U by iU, with $|W| = |U|$.

The excitation anisotropy of the levels a and b in the k-system will be specified, in the general case of alignment, by:

$$N(2q) = \begin{Bmatrix} 1 & 2 & 1 \\ J_a & J_b & J_a \end{Bmatrix} \rho_a(2q) + \begin{Bmatrix} 1 & 2 & 1 \\ J_b & J_a & J_b \end{Bmatrix} \rho_b(2q)$$
$$= (A, iB, C, iB, A). \tag{3}$$

Here, $\{...\}$ stands for the $6j$ symbol, ρ_a and ρ_b are elements of the density matrix for the levels a and b, and A, B, C are real numbers. The symmetry (3) reflects the Hermitian character of the density matrix.

The stationary equations for the non-diagonal elements of that part of the density matrix which depends on the formation of alignment upon excitation, i.e., for the moments of second rank, can be expressed most simply in the H-system:

$$\tilde{R}_{ab}(10) = \frac{1}{L}\left\{-2^{1/2}\tilde{V}(10\tilde{N})(20) + \left(\frac{3}{2}\right)^{1/2}\left[\frac{\tilde{V}(11)\tilde{N}(2-1)}{1-i\varepsilon} + \frac{\tilde{V}(1-1)\tilde{N}(21)}{1+i\varepsilon}\right]\right\},$$
$$\tilde{R}_{ab}(1q) = \frac{1}{L+iq\Delta}\left[\frac{\tilde{V}(1q)\tilde{N}(20)}{2^{1/2}} - \left(\frac{3}{2}\right)^{1/2}\frac{\tilde{V}(10)\tilde{N}(2q)}{1+iq\varepsilon} + 3^{1/2}\frac{\tilde{V}(1-q)\tilde{N}(22q)}{1+2iq\varepsilon}\right],$$
$$q = \pm 1, \quad L = 1 + i\frac{\Omega - \mathbf{kv}}{\Gamma}, \quad \varepsilon = \frac{\mu g H}{\gamma}, \quad \Delta = \frac{\mu g H}{\Gamma}. \tag{4}$$

Here γ is the rate of alignment decay, Γ is the dipole-moment relaxation rate, μg is the coefficient of Zeeman splitting (the g coefficients are taken to be the same for both a and b levels), Ω is the frequency detuning of the radiation with respect to the center of the atomic transition, and $\mathbf{v}$ is the atom velocity. There is no need to solve the total equation, because a moment of rank zero (the total level population) does not generate an OMR with uniform width, and there is practically no orientation on the levels.[8] Since the equation is invariant in the xq representation with respect to rotations, these parts of the density matrix add nothing to (4).

The matrix elements in the k- and H-systems are connected by Wigner's D matrices for a rotation about the y-axis:[9]

$$\begin{aligned}\tilde{R}_{ab}(1q)&=\sum_{q'}D^{1}_{q'q}(\beta)R_{ab}(1q'),\\ \tilde{V}_{ab}(1q)&=\sum_{q'}D^{1}_{q'q}(\beta)V_{ab}(1q'),\\ \tilde{N}(2q)&=\sum_{q'}D^{2}_{q'q}(\beta)N(2q').\end{aligned}\tag{5}$$

To evaluate the optical characteristics, we must transform the non-diagonal elements of the density matrix of the H-system back into the k-system, by means of an reverse rotation. The expressions for the elements $R_{ab}(1q)$ for the excitation of individual alignment components in (3) are:

$$N(2q)=(A,\ 0,\ 0,\ 0,\ A),$$
$$R_y=\frac{3^{1/2}A}{L}\left[\frac{W(1+\varepsilon_\parallel^2)}{1+4\varepsilon^2}-\frac{iU\varepsilon_\parallel(1-2\varepsilon^2+3\varepsilon_\parallel^2)}{(1+\varepsilon^2)(1+4\varepsilon^2}\right],\tag{6}$$

$$R_z=\frac{-3^{1/2}A(W\varepsilon_\parallel+2iU\varepsilon_\parallel^2)(1-2\varepsilon^2+3\varepsilon_\parallel^2)}{L(1+\varepsilon^2)(1+4\varepsilon^2)},$$
$$N(2q)=(0,\ 0,\ C,\ 0,\ 0),$$
$$R_y=\frac{(W-3iU\varepsilon_\parallel)(1+4\varepsilon^2-3\varepsilon_\parallel^2)C}{2^{1/2}L(1+\varepsilon^2)(1+4\varepsilon^2)},\tag{7}$$

$$R_z=-\frac{2iUC}{2^{1/2}L}\left[1-\frac{3\varepsilon_\parallel^2(1+4\varepsilon^2-3\varepsilon_\parallel^2)}{(1+\varepsilon^2)(1+4\varepsilon^2)}\right]$$
$$-\frac{3CW\varepsilon_\parallel(1+4\varepsilon^2-\varepsilon_\parallel^2)}{2^{1/2}L(1+\varepsilon^2)(1+4\varepsilon^2)},$$

$$N(2q)=(0,\ iB,\ 0,\ iB,\ 0),$$
$$R_y=\frac{2\cdot3^{1/2}BW\varepsilon_\parallel}{L(1+4\varepsilon^2)}+\frac{3^{1/2}iBU}{L}f_1(\varepsilon_\parallel,\varepsilon_\perp),$$
$$R_z=\frac{[-2\cdot3^{1/2}iBU\varepsilon_\parallel+3^{1/2}BW]}{L}f_1(\varepsilon_\parallel,\varepsilon_\perp).\tag{8}$$

Here

$$R_z=R_{ab}(10),\quad R_y=\frac{i}{2^{1/2}}[R_{ab}(11)+R_{ab}(1-1)]=\tilde{R}_y,$$
$$f_1(\varepsilon_\parallel,\varepsilon_\perp)=\frac{1+\varepsilon_\parallel^2}{1+\varepsilon_\parallel^2+\varepsilon_\perp^2}-\frac{4\varepsilon_\parallel^2}{1+4\varepsilon_\parallel^2+4\varepsilon_\perp^2},\quad \varepsilon^2=\varepsilon_\parallel^2+\varepsilon_\perp^2,$$
$$\varepsilon_\parallel=\frac{\mu gH_x}{\gamma},\quad \varepsilon_\perp=\frac{\mu gH_z}{\gamma}.$$

In obtaining the formulas (6)–(8) we assumed that $\Gamma\gg\gamma$, which is true for gas atoms because of the important role of their collisions with the other atoms. The optomagnetic birefringence and dichroism S_n and S_a are calculated from the expressions:

$$\begin{aligned}S_a&\propto\mathrm{Re}\,\langle W^*R_y-(iU)^*R_z\rangle_v,\\ S_n&\propto\mathrm{Im}\,\langle W^*R_y-(iU)^*R_z\rangle_v,\end{aligned}\tag{9}$$

where $\langle\ldots\rangle_v$ denotes an average over velocities with a Maxwell distribution.

Let us give the final forms for OMR_a and OMR_n in the case of two types of excitation anisotropy. For axial anisotropy, we have $A=-(3/2)^{1/2}C$ and the OMR structure is

$$S_a^{(1)}\propto\exp\left[-\left(\frac{\Omega}{k\bar{v}}\right)^2\right]\varepsilon_\perp^2\left[F_1(\varepsilon_\parallel,\varepsilon_\perp)-\frac{3\Omega}{k\bar{v}}F_2(\varepsilon_\parallel,\varepsilon_\perp)\right],$$
$$S_n^{(1)}\propto\exp\left[-\left(\frac{\Omega}{k\bar{v}}\right)^2\right]\varepsilon_\perp^2\left[\frac{\Omega}{k\bar{v}}F_1(\varepsilon_\parallel,\varepsilon_\perp)-3F_2(\varepsilon_\parallel,\varepsilon_\perp)\right],$$
$$F_1(\varepsilon_\parallel,\varepsilon_\perp)=\frac{1-4\varepsilon_\parallel^2}{1+4\varepsilon_\parallel^2+4\varepsilon_\perp^2}+\frac{\varepsilon_\parallel^2}{1+\varepsilon_\parallel^2+\varepsilon_\perp^2},$$
$$F_2(\varepsilon_\parallel,\varepsilon_\perp)=\frac{\varepsilon_\parallel}{(1+\varepsilon_\parallel^2+\varepsilon_\perp^2)(1+4\varepsilon_\parallel^2+4\varepsilon_\perp^2)}.\tag{10}$$

For a strictly transverse field, the form of the resonances simplifies considerably and becomes Lorentzian. The OMR_a amplitude is a maximum at the center of the line and decreases symmetrically as Ω increases. The OMR_n amplitude is antisymmetric as a function of Ω, and vanishes at the center of the line. A change of polarization from right circular to left circular does not change the sign of OMR_a but changes the sign of OMR_n, in agreement with (1).

The addition of a longitudinal field complicates the form of the first principal terms of OMR_a and OMR_n. Besides the broadening, the ratio of the amplitudes of the two terms changes, and their widths differ by a factor of two. At the same time there appear supplementary OMR components proportional to $\varepsilon_\parallel$. In OMR_a the increment is antisymmetric in Ω, while in OMR_n it is symmetric. These second terms in (10) have a dispersion symmetry different from that of the first terms. For $\Omega=0$, a variation of the longitudinal field for OMR_n is tantamount to a change of the radiation frequency (see curves *2* and *2'* in Fig. 3).

There are interesting phenomena occurring when $\Omega\neq0$. The OMR_a increment antisymmetric in the longitudinal field influences the total amplitude (see curves *4* and *4'* in Fig. 3). A change of polarization effectively changes the sign of $\varepsilon_\parallel$ and the sign of the increment to OMR_a. In OMR_n, a change of sign of $\varepsilon_\parallel$ is compensated by a change in the sign of the birefringence signal, a fact which in the curves *2* and *2'* of Fig. 3 manifests itself as a shift along the vertical axis, due to the increment of the first term $S_n^{(1)}$ from formula (10). Consequently, the properties of OMR in the case of an axial symmetry are qualitatively equal to those observed experimentally for OMR-1.

The OMR have entirely different properties in the case of axial-symmetry breaking corresponding to (8):

$$S_a^{(2)} \propto \exp\left[-\left(\frac{\Omega}{k\bar{v}}\right)^2\right]\left[\frac{\Omega}{k\bar{v}} f_1(\varepsilon_\parallel, \varepsilon_\perp)+f_2(\varepsilon_\parallel, \varepsilon_\perp)\right],$$

$$S_n^{(2)} \propto \exp\left[-\left(\frac{\Omega}{k\bar{v}}\right)^2\right]\left[f_1(\varepsilon_\parallel, \varepsilon_\perp)+\frac{\Omega}{k\bar{v}} f_2(\varepsilon_\parallel, \varepsilon_\perp)\right],$$

$$f_2(\varepsilon_\parallel, \varepsilon_\perp)=\varepsilon_\parallel\left(\frac{1-4\varepsilon_\parallel^2}{1+4\varepsilon_\parallel^2+4\varepsilon_\perp^2}+\frac{1+\varepsilon_\parallel^2}{1+\varepsilon_\parallel^2+\varepsilon_\perp^2}\right). \quad (11)$$

The resonances have now different amplitude-dispersive properties. In the absence of a longitudinal field, the birefringence signal is a maximum at the center of the line and decays symmetrically away from the center. In contrast to this, the dichroism signal vanishes at the center of the line, and has different signs in the blue and red wings of the line. If one uses in the averaging a distribution with a "shelf," the OMR_n acquires a dependence on frequency, and OMR_a vanishes in a certain frequency range. The experimental data make such a distribution quite plausible. In this case, one may neglect the first term in $S_a^{(2)}$ and the second term in $S_n^{(2)}$. Then, when $\varepsilon_\parallel = 0$, the form of OMR_n becomes purely Lorentzian, but OMR_a vanishes. Weak longitunal fields complicate the structure of OMR_n, which is now given by a linear combination of two Lorentzians with widths one twice as large as the other. As a consequence of this structure, for sufficiently large $\varepsilon_\parallel$, a dip twice as narrow appears in the center of the broad OMR_n. When recording by using the derivative method, one will observe a component of opposite sign, just as in curves *1*, *2*, *5* showed in Fig. 2.

When $|\varepsilon_\parallel| > 0$, there appears a dichroism resonance with an amplitude proportional to the longitudinal field. It can be easily seen that the resultant OMR_a is initially narrower than OMR_n. There exists an optimum longitudinal field for the observation of OMR_a, beyond which the amplitudes of both OMR_n and OMR_a decrease rapidly, because of the broadening effect of the field. The propotionality of the OMR_a amplitude to the longitudinal field, its broadening effect, and the non-uniformity of the laboratory longitudinal field lead to a nonmonotonic dependence of the width on $\varepsilon_\parallel$, as shown in Fig. 4.

The OMR structure is also related to a polarization symmetry. Both OMR_a and OMR_n in (11) must change sign when the polarization is changed from right-circular to left-circular. OMR_n changes sign according to (1) as is normal in birefringence, while OMR_a changes sign because $\varepsilon_\parallel$ effectively changes sign.

4. CONCLUSIONS

As we have shown, the properties of the resonances (10) are qualitatively those observed experimentally for OMR-1. The anomalous amplitude-dispersive and polarization properties of the resonances (11) also agree with the data on OMR-2. As a most plausible working hypothesis we should consider the following. OMR-1 are generated by anisotropic excitation with axial symmetry corresponding to the experimental geometry. In order to form OMR-2, one needs for the working levels another quantum state, as given by (8). In Cartesian coordinates, such a state is described by an excitation tensor with nonvanishing nondiagonal *z*- and *y*-components. Experiments involving a change in orientation of the transverse magnetic field, made by rotating the electromagnet through $\pm 22.5°$, showed that the OMR-2 amplitude remains practically unchanged. Therefore, the excitation tensor does not reduce to diagonal form, and one could speak about an excitation of a state with helicity. The narrowness of the resonances is indicative of the virtuality of such a state for the levels $3s_2$ and $2p_4$, which serve only as intermediaries for a long-lived unknown source. The usefulness of such a representation was demonstrated[10] in the case of alignment.

As possible long-lived sources of excitation in neon one might consider[5] the metastable levels $1s_3$ and $1s_5$, as well as the quasimetastable levels $2s_3$ and $2s_5$. The levels $1s_3$ and $2s_3$ have zero angular momentum and cannot be excited anisotropically, but the levels $1s_5$ and $2s_5$ have an angular momentum *J*-2, and could play the role of sources. However, one needs a process which, in the absence of external magnetic fields, could prepare a state with helicity, or transform an axially symmetric state into such a state.

One could assume that transfer of alignment from a metastable state produces a nonequivalent mixing of states with right or left symmetry. This might be a manifestation of parity nonconservation in atomic transitions, but this is a rather daring hypothesis.

The authors thank S. G. Rautian and A. M. Shalagin for valuable discussions and interest in this work, L. V. Il'ichev for useful remarks and advice, and C. N. Atutov for reviewing the results.

[1] É. G. Saprykin, S. N. Seleznev, and V. A. Sorokin, *Abstracts, Second All-Union Seminar on Optical Orientation of Atoms and Molecules,* [in Russian], Leningrad Inst. of Nucl. Physics, 1989.
[2] É. G. Saprykin, S. N. Seleznev, and V. A. Sorokin, Pis'ma Zh. Eksp. Teor. Fiz. **50**, 316 (1989) [JETP Lett. **50**, 351 (1989)].
[3] Ch. E. Moore, *Atomic Energy Levels*, Nat. Bur. Stand., 1949.
[4] G. N. Nikolaev, S. G. Rautian *et al.*, Opt. Spektrosk. **60**, 244 (1986) [Opt Spectrosc. (USSR) **60**, 428 (1986)].
[5] W. R. Bennet and P. J. Kindelman Jr., Phys. Rev. **149**, 38 (1966).
[6] S. A. Kazantsev, Usp. Fiz. Nauk **139**, 621 (1983) [Sov. Phys. Usp. **26**, 328 (1983)].
[7] S. G. Rautian, G. I. Smirnov, and A. M. Shalagin, *Nonlinear Resonances in the Spectra of Atoms and Molecules* [in Russian], Nauka, Novosibirsk, 1979.
[8] T. Manabe, T. Yabuzaki, and T. Ogawa, Phys. Rev. Lett. **46**, 637 (1981).
[9] L. C. Biedenharn and J. D. Louck, *Angular Momentum in Quantum Physics*, Cambridge, 1984.
[10] M. P. Chaĭka, *Interference of Degenerate States* [in Russian], Izd. Len. Gos. Univ., 1975.

Translated by C. Eftimiu